Journal of the Nigerian Association of Mathematical Physics
***Volume* 15 (November, 2009), pp 197 - 204**

The use of source and Green's functions to model pressure distribution in a bounded layered reservoir with lateral wells, Part II: General solutions

E. S. Adewole
Department of Petroleum Engineering;
University of Benin, Benin City, Nigeria.

Abstract

In this paper, solutions to the mathematical models in Part I of this title are derived. Appropriate flow period delineation methods are discussed. Results show that as an enlarged reservoir, flow attains pseudosteady state at late times when reservoir dimensionless pressure is inversely proportional to the reservoir dimensionless external lengths and directly proportional to dimensionless flow time. Furthermore, only superposition in time can be used to account for complete dimensionless pressure history. Finally, flow periods delineation makes it possible for individual layer dimensionless pressures to be quantified and therefore permits individual layer characterization.

Nomenclature
A = external dimension along x-axis, *ft*;
b = external dimension along y-axis, *ft*;
$p_D = \dfrac{kh\Delta p}{141.2q\mu B}$;
$t_D = \dfrac{0.001056kt}{\mu\phi c_t L^2}$;
$i_D = \dfrac{2i}{L}\sqrt{\dfrac{k}{k_i}}$ i = positions along x or y or z axes, *ft*;
$h_D = 1/L_D$; Δ = drop;
p = pressure, psi;
k = permeability, *md*;
h = pay thickness, ft;
t = time, hours;
q = flow rate, STB/Day;
μ = oil viscosity, cp;
B = oil formation volume factor, bbl/STB;
c_t = total fluid compressibility, 1/psi;
L = well length, ft;
erf = error function;
τ = dimensionless dummy time variable.

Subscripts
x, y, z = x, y, or z, directions;
D = dimensionless;
w = wellbore;
e = external

1.0 Introduction

In Part I of this title [1], only mathematical models are derived. In this concluding part, solutions to the mathematical models are now presented. Although, there can be more flow periods, only two major flow periods will be delineated, these are (1) the infinite-acting flow period and (2) the period during which the interface is felt. These are the periods needed for transient flow test analyses and layers cossflow characterization. It should be noted that only a

e-mail address: steveadewole@yahoo.com
Telephone: +234-08039237561

bounded reservoir with crossflow layers are considered. All dimensionless parameters and detailed reservoir description appear in [1].

2.0 Early radial (infinite-acting) flow period pressure distribution approximations

During this period, the reservoir pressure changes rapidly at inception of a new transient regime. In general, if we consider the early times as very small, then [2] shows that

$$p_D = -\frac{\alpha h_D}{8}\sqrt{\frac{kk}{k_y k_z}}\int_x^{\infty}\frac{e^{-u}}{u}du \tag{2.1}$$

where

$$x = \frac{R_D^2}{4t_D}$$

and

$$R_D^2 = (y_D - y_{wD})^2 + (z_D - z_{wD})^2,$$

or

$$p_D = -\frac{\alpha h_D}{8}\sqrt{\frac{kk}{k_y k_z}}Ei(-x). \tag{2.2}$$

where $\alpha = 2$ for $x_D < \sqrt{k/k_x}$, 1 for $x_D = \sqrt{k/k_x}$, and 0 for $x_D > \sqrt{k/k_x}$, for an anisotropic reservoir.

Equation 2.2 describes the dimensionless pressure distribution when the reservoir is infinite-acting and applies to any layer of the reservoir. It prevails until curbed by boundary effects. The dimensionless time, t_D, is the dimensionless flow time of interest. This flow period occurs in all reservoirs irrespective of size.

2.1 Early linear period pressure distribution approximations

When there is crossflow between layers, the entire reservoir behaves as one enlarged reservoir, especially when the entire length of the interface is permeable. Early linear flow period manifests when the nearest boundary (reservoir or wellbore) is felt, and the dimensionless pressure approximation will be considered under the following instances of production/injection of fluid from/into Layer 1.

2.1.1 Layer 1 still being produced or injected

Flow transients have moved beyond the wellbore in Layer 1 but have not felt the impact of the crossflow interface. The total dimensionless pressure distribution in this case is obtained as a superposition of the dimensionless pressure during infinite behaviour and the dimensionless pressure at the inception of initial transient but before the interface is felt. That is,

$$p_D = -\frac{\alpha h_{D1}}{8}\sqrt{\frac{k_1 k_1}{k_{y1}k_{z1}}}Ei(-x) + \frac{\sqrt{\pi}E_1}{2}\sqrt{\frac{k_1}{k_{y1}}}\int_{t_{De}}^{t_{Dz}}\left[erf\left(\frac{\sqrt{k_1/k_{x1}}+x_{D1}}{2\sqrt{\tau}}\right)+erf\left(\frac{\sqrt{k_1/k_{1x}}-x_{D1}}{2\sqrt{\tau}}\right)\right]\cdot$$

$$\frac{e^{-\frac{(y_{D1}-y_{wD1})^2}{4\tau}}}{\sqrt{\tau}}\cdot\sum_{n=1}^{\infty}\exp\left(-\frac{(2n+1)^2\pi^2\tau}{4h_{D1}^2}\cos(2n+1)\pi\frac{z_{D1}}{h_{D1}}\cos(2n+1)\pi\frac{z_{wD1}}{h_{D1}}d\tau\right. \tag{2.3}$$

where

$$z_{D1}+z_{wD1}+2r_{wD1} < h_{D1},$$

and z_{D1} is an arbitrary position within Layer 1, along the z-axis.

2.1.2 Layer 1 top boundary felt by production or injection

Flow transients have now moved very far beyond Well 1 and at the interface. Accordingly, the total dimensionless pressure distribution is obtained as

$$p_D = -\frac{\alpha h_{D1}}{8}\sqrt{\frac{k_1 k_1}{k_{y_1} k_{z1}}}Ei(-x) + \frac{\sqrt{\pi}E_1}{2}\sqrt{\frac{k_{11}}{k_{y_1}}}\int_{t_{De}}^{t_{tDzf}}\left[erf\left(\frac{\sqrt{k_1/k_{x1}}+x_{D1}}{2\sqrt{\tau}}\right)+erf\left(\frac{\sqrt{k_{11}/k_{x1}}-x_{D1}}{2\sqrt{\tau}}\right)\right]\cdot$$

$$\frac{e^{-\frac{(y_{D1}-y_{wD1})^2}{4\tau}}}{\sqrt{\tau}}\cdot\sum_{n=1}^{\infty}\exp\left(-\frac{(2n+1)^2\pi^2\tau}{4h_{D1}^2}\cos(2n+1)\pi\frac{h_D - z_{wD1}}{h_{D1}}\cos(2n+1)\pi\frac{z_{wD1}}{h_{D1}}d\tau\right. \qquad (2.4)$$

where t_{Dzf} is the dimensionless time the interface is felt. The difference between the dimensionless times t_{Dz} and t_{Dzf} may be so small that it could be neglected thus making the period from t_{Dz} to t_{Dzf} indistinguishable in practice. This period (when the interface is felt) may not occur if

(1) the interface is very permeable throughout its entire length
(2) fluid passes through the interface at very high rate, and
(3) the reservoir layers have high vertical permeabilities

2.1.3 Layer 2 now being produced or injected

The moment fluid in Layer 2 is being produced or injected, pressure gradient are expected to fall, if the permeability of Layer 1 is greater than that of Layer 2, and vice versa. This is as a result of fluid equilibrium readjustment. For more than two layers, this change in pressure gradient will characterize depletion or injection of each new layer. The total dimensionless pressure distribution is therefore given as the sum of the dimensionless pressure since Well 1was put on production or injection and the dimensionless pressure created in Layer 2 since the interface had been felt. That is,

$$p_{D1} = -\frac{\alpha h_D}{8}\sqrt{\frac{k\,k}{k_Y k_z}}Ei\left(\frac{R^2{}_D}{4\beta t_D}\right)+\frac{\sqrt{\pi\beta}E}{2}\sqrt{\frac{k}{k_y}}\int_{t_{Dfe}}^{t_D}\left[erf\left(\frac{\sqrt{k/k_x}+x_D}{2\beta\tau}\right)+erf\left(\frac{\sqrt{k/k_x}-x_D}{2\beta\tau}\right)\right]\bullet$$

$$\frac{e^{-\frac{(y_D-y_{wD})^2}{4\beta\tau}}}{\sqrt{\tau}}\cdot\sum_{n=1}^{\infty}\exp\left(-\frac{(2n+1)^2\pi^2\beta\tau}{4h_D^2}\cos(2n+1)\pi\frac{h_{D-Z_{wD1}}}{h_D}\cos(2n+1)\pi\frac{z_{wD1}}{h_D}d\tau\right. \qquad (2.5)$$

where $\beta = (\mu_1\phi_1 c_{t\,1}L_1^2k_2)/(\mu_2\phi_2 c_{t\,2}L_2^2k_1)$, and E is defined in [1] for several flow periods. All reservoir properties are now average of the two layers properties. Equation (3.5) takes into account the fact that Well 1 is still used as the production or injection well and ($\beta\tau$) is the dimensionless time since Layer 2 started responding to production/injection in Well 1. It should be noted that the entire vertical thickness of the reservoir h_D is now exposed to flow. For vertically stacked layers,

$$y_D^2 = x_D^2 + z_D^2 \qquad (2.6)$$

The same derivation procedure is applicable if Well 2 is used as the monitoring well.

Late Intermediate Linear Flow Dimensionless Pressure Approximations for Individual Layers. The chances that any of the early linear pressure distributions given by (3.3 to (3.5) will occur depend on

(1) the thickness of the reservoir in relation to the length of the producing wellbore,
(2) the vertical-to-horizontal permeability ratio, and
(3) the production or injection rate of fluid from Well 1.

If the wellbore length is short compared to the reservoir thickness, the early time radial periods may not occur for long. Rather, the lateral ends of the well will be felt earlier giving rise to an early linear flow period, while the transient in the vertical direction will still be exhibiting infinite behavior. On the other hand, if the formation is thinner than the length of the wellbore, then the early time linear behavior will be noticed earlier than the ends of the wellbore are felt. During this late intermediate flow period dimensionless pressure distribution approximations are written as

$$p_{D1}(x_{D1},Y_{D1},z_{D1})=\frac{E\sqrt{\pi}}{a_{D1}}\sqrt{\frac{k}{k_y}}\int_{t_{De}}^{t_D}\left[1+\frac{4a_{D1}}{\pi}\sum_{n=1}^{\infty}\frac{1}{n}\exp\left(-\frac{n^2\pi^2 t_D}{a^2{}_{D1}}\right)\sin(\frac{n\pi}{a_{D1}})\cos(n\pi\frac{x_{D1}}{a_{D1}})\cos(n\pi\frac{x_{D1}}{a_{D1}})\right]$$

$$\frac{e^{-\frac{y_{D1}-y_{wD1})^2}{4\tau}}}{\sqrt{\tau}}\bullet\sum_{n=1}^{\infty}\exp(-\frac{(2n+1)^2\pi^2\tau}{4h_{D1}^2})\cos((2n+1)\pi\frac{z_{wD1}}{h_{D1}})\cos((2n+1)\pi\frac{z_{D1}}{h_{D1}})d\tau-\frac{\alpha h_{D1}}{8}\sqrt{\frac{kk}{k_yk_z}}Ei(-\frac{R^2{}_{D1}}{4t_D}) \quad (2.7)$$

for Layer 1, and

$$p_{D1}(x_{D1},Y_{D1},z_{D1})=\frac{E\sqrt{\pi\beta}}{a_{D2}}\sqrt{\frac{k}{k_y}}\int_{t_{De}}^{t_D}\left[1+\frac{4a_{D2}}{\pi}\sum_{n=1}^{\infty}\frac{1}{n}\exp\left(-\frac{n^2\pi^2\tau\beta}{a^2{}_{D2}}\right)\sin(\frac{n\pi}{a_{D2}})\cos(n\pi\frac{x_{wD2}}{a_{D2}})\cos(n\pi\frac{x_{D2}}{a_{D2}})\right]$$

$$\frac{e^{-\frac{y_{D2}-y_{wD2})^2}{4\tau\beta}}}{\sqrt{\tau}}\bullet\sum_{n=1}^{\infty}\exp(-\frac{(2n+1)^2\pi\beta\tau}{4h^2{}_{D2}})\sin((\frac{2n-1}{2})\pi\frac{z_{wD2}}{h_{D2}})\sin((\frac{2n-1}{2})\pi\frac{z_{D2}}{h_{D2}})d\tau-\frac{\alpha h_{D2}}{8}\sqrt{\frac{kk}{k_yk_z}}Ei(-\frac{R^2{}_{D2}}{4\beta t_D}) \quad (2.8)$$

for Layer 2.

2.1.5 Late and final linear dimensionless pressure distribution

During this period all the external boundaries have been felt, and thus, since the external boundaries are all sealed, pseudosteady flow now prevail through out the production life of the well. This is the case if one well is used for pressure monitoring**.**

Using Equation (22) of [1], the late and final dimensionless pressure distributions for the layers are written approximately as

$$p_{D2}(x_{D2},y_{D2},z_{D2},\tau)=\frac{2\pi E_1}{a_{D2}b_D}\int_{t_{De}}^{t_D}\left[\sum_{n=1}^{\infty}\exp(-\frac{(2n+1)^2\pi^2\tau}{4h_{D1}^2})\cos(2n+1)\pi\frac{z_{wD1}}{h_{D1}}\cos(2n+1)\pi\frac{z_{D1}}{h_{D1}}\right]d\tau \quad (2.9)$$

for Layer 1, and

$$p_{D2}(x_{D2},y_{D2},z_{D2},\tau)=\frac{2\pi E_2}{a_{D2}b_{21}}\int_{t_{De}}^{t_D}\left[\sum_{n=1}^{\infty}\exp(-\frac{(2n-1)^2\pi^2\beta\tau}{4h_{D2}^2})\sin((\frac{2n-1}{2})\pi\frac{z_{wD2}}{h_{D2}})\sin((\frac{2n-1}{2})\pi\frac{z_{D2}}{h_{D2}})\right]d\tau. \quad (2.10)$$

for layer 2. Obviously, (2.9) and (2.10) could yield a final steady state period, if the interface is long, reasonably permeable and is felt first. Otherwise, infinite-acting flow continues to prevail. If a steady state is eventually achieved it may be irreversible if any of these layers is experiencing highly compressible fluid recharge. Note however, that (2.9) and (2.10) do not show complete history, which can be obtained by superposition of (2.9) and (2.10) with equivalent infinite-acting expressions.

3.0 Flow periods determination

Several flow periods may exist in each of the horizontal wells. The number of periods and their duration depend strongly on the wellbore geometry, reservoir properties and well flow rates.

For a given reservoir thickness the times required for pressure transient to reach the vertical boundaries is derived according to Odeh and Babu [3] as

$$t_{z(1\%\ error)} = 0.536\alpha d^2_z/k_z \tag{3.1}$$

For the nearest vertical boundary

$$d_z \equiv \min(z_w, h\text{-}z_w) \tag{3.2}$$

and for the farthest vertical boundary

$$D_z \equiv \max(z_w, h\text{-}z_w) \tag{3.3}$$

where

$$\alpha = 157.952\phi\mu c_t \tag{3.4}$$

With reference to Figure 3.1, these times can be written as

$$t_{Dzf} \approx 85(h_{D1} - z_{D1)})^2 \tag{3.5}$$

for Well 1 and

$$t_D \approx 85z^2{}_{wD2} \tag{3.6}$$

for Well 2.

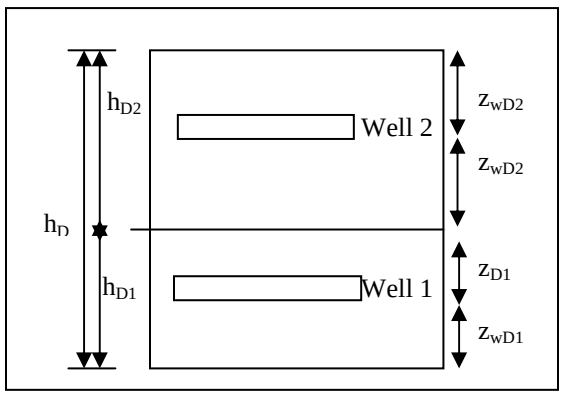

Figure 3.1: Well arrangement model in the layers

In the same manner, the top-most no-flow boundary is felt from Well 1 at dimensionless time given as

$$t_D \approx 85(h_{D1} - z_{D1)})^2 \tag{3.7}$$

and

$$t_D \approx 85z^2{}_{wD2} \tag{3.8}$$

for Well 2.

4.0 Computation of well responses

Integration with respect to position as encountered in the expression for E is performed analytically. But all integration with respect to time can be evaluated numerically using two methods, viz.: (1) the Gauss-Laguerre quadrature and (2) the Gauss-Legendre quadrature [4, 5]. The first method can be used to evaluate the associated exponential integrals at early times. The Gauss-Legendre quadrature is very useful in computing dimensionless pressures after the expiration of the early radial (infinite-acting) flow period. Associated errors were not quantified where these quadratures were applied as they are not capable of affecting overall results according to [5].

Apart from (3.5) and (3.8), some knowledge of t_{DZf} can also be either estimated from observed changes in gradients on p_{WD} versus log t_D plot long after the expiration of the early radial period or as follows:

$$t_{Dzfj} \le \max\begin{cases} 100/(\pi L_{Dj}^2 \\ 25\left[(x_{Dj} - \sqrt{k/k_2})^2 + y_{Dj}^2\right] \\ 25\left[(x_{Dj} + \sqrt{k/k_2})^2 + y_{Dj}^2\right] \end{cases} \tag{4.1}$$

This time suggests that flow has moved entirely away from the *x*-*z*-plane of Layer *j* and now in the *x*-*z*-plane of Layer *j* + 2, depending on the layer of interest. In a layered reservoir t_{Dzf} may be compared to long time flow period for a particular layer. Equations (3.5) and (3.6) provide an upper limit check on t_{Dz} and they indicate that the interface had been felt since t_{Dzf}. t_{Dzf} values enable correct computation and analysis of well flow pressures to be done.

At $t_D > t_{Dzf}$ flow transients are in another portion of the reservoir. To be sure of the location, if t_{Dzf} is known, then calculate t_{Dzfj} , the dimensionless time for the pressure transient to have gone beyond the interface and now at any point in Layer *j* or (*j* + 1). For Layer 1,

$$t_{Dzf1} \cong 85(h_D - h_{D1})^2 \tag{4.2}$$

and for Layer 2, t_{Dzf2} is calculated from (3.6).

If t_{Dzf1} is greater than t_{Dzf} then depending on the layer of interest a portion outside the interface is exposed to flow. In a layered reservoir with crossflow, if Well *j* is used to monitor pressure distribution then early time flow will last for as long as given below:

$$t_{Dej} \le \min\begin{cases} \delta_{Dj}^2/20 \\ (z_{Dj} + z_{wD})^2/20 \\ (z_{Dj} + z_{wD} - 2)^2/20 \end{cases} . \tag{4.3}$$

where

$\delta_{Dj} = \sqrt{k/k_x} - x_{Dj}$ if $\sqrt{k/k_x} > x_{Dj}$ and $\delta_{Dj}=2\sqrt{k/k_x}$ if $\sqrt{k/k_x} = x_{Dj}$.

It should be noted that $h_{Dj} \le z_{Dj}+z_{wDj} < h_D$. For the same crossflow layers, given Well *j*, long time pressure distribution is obtained in the reservoir at dimensionless time given approximately as

$$t_{Dej} \ge \max\begin{cases} 100/(\pi L_{Dj}^2 \\ 25\left[(x_{Dj} - \sqrt{k/k_x})^2 + y_{Dj}^2\right] \\ 25\left[(x_{Dj} + \sqrt{k/k_x})^2 + y_{Dj}^2\right] \end{cases} \tag{4.4}$$

The periods given by these expressions are approximate. Fairly accurate periods can be confirmed from plots of $p_{w\,D}$ versus t_D and on pressure derivative plots.

To simulate an infinite-conductivity wellbore, take x_{Dj} = 0.732, but $0 \le x_{Dj} \le 1.0$ represent uniform flux wellbore. Specifically, x_{Dj} = 0.0 represents fluid flow measurement at the well "elbow" and x_{Dj} = 1.0 gives pressure distribution at the well tip or well "toe".

Finally, because Layers 1 and 2 may have quite different reservoir and wellbore properties, it is provided that the response time of Layer 2 is some multiple, β, of Layer 1. In other words, if a comparison between Layers 1 and 2 is to be made in terms of pressure behaviour, then this factor has to be used to establish a basis for comparison. The factor accounts for flow time between layers as a result of layering in the reservoir.

When interlayer flow cases are considered, for example, in enhanced oil recovery (EOR) projects the actual values of β are calculated for a given set of reservoir fluid and wellbore properties. In all computations *n*, 1, and m should be assumed to be unity, i.e., near the wellbore. For early times, our results are compared with some authors' results [6], [7] and [8] as shown in Table 4.1 below.

Table 4.1: Comparison of results of some authors for dimensionless Wellbore pressure
$x_D = 0.732$, $y_{wD} = 0.0005$, $h_D = 0.1$

t_D	**Ref. [7]**	**Ref. [8]**	**Ref. [9]**	**Our Results**
0.000001	0.05490	0.05472	0.05507	0.05489
0.00001	0.1124	0.1126	0.11245	0.11245
0.0001	0.17007	0.1700	0.11260	0.17001
0.001	0.22888	0.2288	0.17098	0.22758
0.01	0.34958	0.3495	0.29164	0.29547
0.1	0.66767	0.6675	0.60972	0.66853
1	1.37630	1.3760	1.31828	1.34005

There is close agreement with other authors' results. The slight difference occurring at late dimensionless times is probably due to differences in choices of numerical methods and in the yardstick for delineating flow periods. Like earlier remarked, only plots of observed dimensionless pressures against dimensionless time can reliably reveal the commencement and end of flow boundaries.

5.0 Conclusion

Mathematical models describing pressure in a bounded layered reservoir with lateral wells have been solved. Results obtained from numerical computation show

That pressure distributions are the same for all layers of the reservoir at early times, if the layers and wellbore properties are the same.

(1) The interface effect is actually felt later than the infinite–acting period.

(2) Regional dimensionless pressure distribution can be estimated for each layer even with cross flow interface, if flow boundaries are reliably delineated.

(3) Well design and completion strongly affect the performance of a layered reservoir with crossflow.

(4) Superposition in time is the only way of accounting for complete dimensionless pressure history.

References

[1] Adewole, E.S.: "The Use of Sources and Green's Functions to Model Pressure Distribution in a Bounded Reservoir with Lateral Wells; Part I: Mathematical Derivations" *Abacus: The J. of the Mathematical Ass. of Nigeria*, vol. 33, Number 2B, Mathematical Series, Sept. 2006, p. 436 – 450.

[2] Ozkan, E., Raghavan, R. and Joshi, S.D.: "Horizontal Well Pressure Analysis," *SPEFE* (Dec. 1989) p. 567 – 575.

[3] Odeh, S.A. and Babu, D.K.: "Transient Flow Behaviour of Horizontal Wells: Pressure Drawdown and Buikdup Analysis," *SPEFE* (March 1990), p.7 – 15, *Trans*., AIME, 289.

[4] Adewole, E.S.: "The Use of Gauss-Legendre and Gauss-Laguerre Quadratures in Solving Problems involving Oil Flow in Horizontal Wells, *Abacus: J. of the Mathematical Ass. of Nigeria*, vol. 34, Number 2B, Mathematical Series, Sept. 2007, p. 380-386.

[5] Carnahan, B. Luther, H.A. and Wilkes, J.O.: "Applied Numerical Methods, John Wiley and Sons Publishers, New York, 1969.

[6] Clonts, M.D. and Ramey, H.J. Jr.: "Pressure-Transient Analysis for Wells with Horizontal Drainholes," paper SPE 15116 presented at the 1986 SPE California Regional Meeting, Oakland, April 2 – 4.

[7] Malekzadeh, D.: "Interference Testing of Horizontal Wells, Ph.D. Dissertation, the Univ. of Oklahoma, Norma, Oklahoma, 1991.

[8] Ozkan, E. and Raghavan, R.: "Performance of Horizontal Wells Subject to Bottom Water Drive," *SPERE* (Aug. 1990) p. 375 – 383, *Trans*., 289.